Structure of saposin A lipoprotein discs

Konstantin Popovic[a], John Holyoake[b,c], Régis Pomès[b,d], and Gilbert G. Privé[a,c,d,1]

[a]Department of Medical Biophysics, University of Toronto, Toronto, ON, Canada M5G 2M9; [b]Molecular Structure and Function, Hospital for Sick Children, Toronto, ON, Canada M5G 1X8; [c]Ontario Cancer Institute, Campbell Family Institute for Cancer Research, Toronto, ON, Canada M5G 1L7; and [d]Department of Biochemistry, University of Toronto, Toronto, ON, Canada, M5S 1A8

Edited by Donald Engelman, Yale University, New Haven, CT, and approved December 17, 2011 (received for review September 23, 2011)

The saposins are small, membrane-active proteins that exist in both soluble and lipid-bound states. Saposin A has roles in sphingolipid catabolism and transport and is required for the breakdown of galactosylceramide by β-galactosylceramidase. In the absence of lipid, saposin A adopts a closed monomeric apo conformation typical of this family. To study a lipid-bound state of this protein, we determined the crystal structure of saposin A in the presence of detergent to 1.9 Å resolution. The structure reveals two chains of saposin A in an open conformation encapsulating 40 internally bound detergent molecules organized in a highly ordered bilayer-like hydrophobic core. The complex provides a high-resolution view of a discoidal lipoprotein particle in which all of the internalized acyl chains are resolved. Saposin A lipoprotein discs exhibit limited selectivity with respect to the incorporated lipid, and can solubilize phospholipids, sphingolipids, and cholesterol into discrete, monodisperse particles with mass of approximately 27 kDa. These discs may be the smallest possible lipoprotein structures that are stabilized by lipid self-assembly.

protein-lipid complex | X-ray crystallography | molecular dynamics | Krabbe disease

Sphingolipid activator proteins (SAPs) are nonenzymatic proteins that are required for the lysosomal breakdown of certain sphingolipids by hydrolase enzymes (1). In general, the SAPs are thought to act by modifying the physical states of the target lipids so that the substrates become accessible to the active sites of the enzymes. The details of how this effect is achieved are not clear, but it is likely that different SAPs use different mechanisms in activating one or more specific lipid/enzyme reactions (2–4). Human lysosomes contain five SAPs: the GM2 activator and the saposins A, B, C, and D. The four homologous saposins are small cysteine-rich α-helical glycoproteins that are derived from the prosaposin precursor protein (5, 6). Saposin A activates the hydrolysis of galactosylceramide by β-galactosylceramidase to produce ceramide and galactose (7, 8). Loss of functional saposin A results in a variant form of Krabbe disease, which is characterized by demyelination, loss of oligodendrocytes, and infiltration of globoid cells (9–12). Saposin A is also important for the loading of lipid antigens onto CD1d molecules (13, 14).

We previously reported the crystal structure of the soluble form of saposin A in the absence of bound lipids (15). In this structure, the small 81 residue protein adopts the compact, monomeric four α-helix closed form of the fold seen in other saposins and saposin-like proteins (15–18). Helices 1 and 4 are disulfide linked in a stem structure, whereas helices 2 and 3 are disulfide linked to each other and form a helical hairpin. In the closed form, the stem and hairpin segments collapse onto themselves, burying the hydrophobic surfaces of the four amphipathic helices via bends at the short turns at the $\alpha1/\alpha2$ and $\alpha3/\alpha4$ junctions. Notably, the closed form of the saposin fold buries the majority of the hydrophobic surfaces into a small hydrophobic core and does not form a cavity that can accommodate lipids. In addition, the external surface of the closed conformation of saposin A is polar and does not have any extended nonpolar regions that would suggest a membrane-active protein. Overall, the lipid-free structure of saposin A provides only limited insight into the lipid interaction properties of saposin A and does not explain how it functions to activate the sphingolipid hydrolysis reaction. However, structural flexibility is a crucial feature for the membrane surface binding and lipid-solubilizing abilities of the saposin proteins (3, 18, 19).

Here, we characterize the interactions of saposin A with various amphiphiles. Saposin A undergoes a conformational change in the presence of lipids and detergents and forms small lipoprotein particles with a wide range of lipids. The 1.9 Å crystal structure of saposin A in complex with zwitterionic detergent lauryldimethylamine-*N*-oxide (LDAO) reveals two saposin chains in an open state forming an amphipathic protein belt surrounding 40 ordered detergent molecules. The structure of the saposin A lipoprotein discs is further supported by coarse-grained molecular dynamics simulations. Overall, we find that saposin A/lipid assemblies form unusual lipoprotein complexes that share some similarities with discoidal high density lipoprotein particles, but are significantly smaller.

Results and Discussion

Characterization of Saposin A with Amphiphiles. To describe the lipid-induced conformational changes in the structure of human saposin A, we used intrinsic tryptophan fluorescence spectroscopy and monitored amphiphile-induced spectral shifts. All solution experiments were conducted at pH 4.8, reflective of the pH within lysosomes. Saposin A contains a single tryptophan, W37, which is solvent exposed in the closed monomeric form. Incubation of saposin A with liposomes resulted in an increase in the intensity of the tryptophan emission spectrum and a 6–8 nm blue shift, indicative of a reduction in the solvent accessibility of the residue and a shift to a less polar environment (Fig. 1*A*). This effect was seen with liposomes made from a wide variety of lipids and lipid mixtures. We also found that several nondenaturing detergents, including LDAO, induced similar spectral shifts. The characteristic changes occurred at concentrations above the critical micelle concentration of the detergent.

Saposin A interacts with liposomes and immobilized lipids (20) but does not remain bound to liposomes (21), suggesting that the protein can form soluble lipid complexes. We incubated liposomes of varying composition with saposin A and analyzed the solutions by size exclusion chromatography (SEC). We consistently observed a single sharp peak in the 35–45 kDa range of the column, corresponding to hydrodynamic radii ranging from 3.07–3.45 nm (Fig. 1*B*, Fig. S1, Table S1). Collectively, we refer to these species as 3.2-nm particles. An additional absorbance peak at the void volume of the column was occasionally detected but did not contain significant amounts of protein and was due to light scattering from large lipid vesicles (Fig. S1). The exact size of

Author contributions: K.P., J.H., R.P., and G.G.P. designed research; K.P. and J.H. performed research; K.P., J.H., R.P., and G.G.P. analyzed data; and K.P., J.H., R.P., and G.G.P. wrote the paper.

The authors declare no conflict of interest.

This article is a PNAS Direct Submission.

Data deposition: Crystallography, atomic coordinates, and structure factors have been deposited in the Protein Data Bank, www.pdb.org (PDB ID code 4DDJ).

[1]To whom correspondence should be addressed. E-mail: prive@uhnres.utoronto.ca.

This article contains supporting information online at www.pnas.org/lookup/suppl/doi:10.1073/pnas.1115743109/-/DCSupplemental.

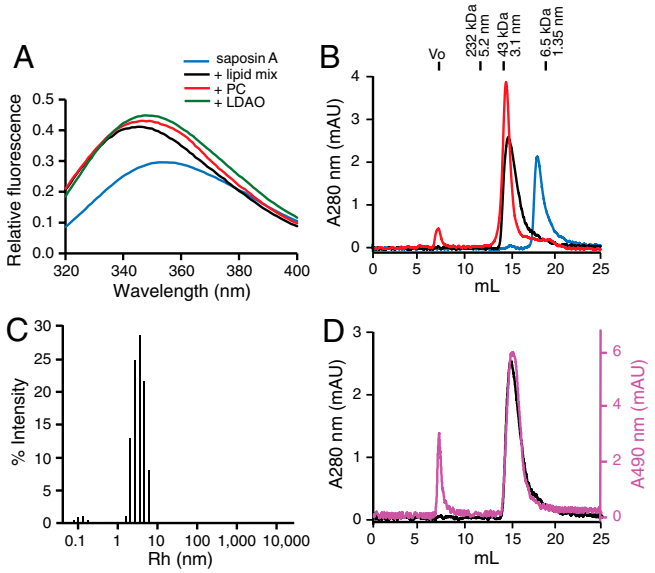

Fig. 1. Solution characterization of saposin A in the presence of lipids and detergent. (*A*) Emission spectra of saposin A in the absence of lipid or detergent (blue), in the presence of a lipid mix designed to mimic lysosomal lipids (PC:Chol:BMP:GalCer 50:25:20:5, lipid mix) (black), PC liposomes (red), or LDAO detergent (green). (*B*) SEC of saposin A in the absence of lipid (blue), after incubation with a 10-fold molar excess of lipid mix (black) or 10-fold molar excess of egg PC liposomes (red). Size standards are indicated above the elution profiles in hydrodynamic radii (nanometers) and mass (kilodalton). (*C*) Size distribution of the pooled and concentrated fractions corresponding to the peak at approximately 15 mls with the lipid mix in *B* as measured by DLS. (*D*) SEC elution profiles from a 10:1 lipid mix:saposin A solution at 280 nm (black) and for an equivalent mix in which the GalCer is replaced with TopFluor-GalCer and absorption monitored at 490 nm (purple).

the 3.2-nm particles was only moderately affected by the lipid to protein molar ratio and the composition of the liposomes (Fig. S1, Table S1). In all cases, a single peak was observed in this size range, indicating a relatively narrow distribution of species. We observed similar 3.2-nm particles regardless of whether or not anionic phospholipids, cholesterol, or glycosphingolipids were present in the liposomal mixtures (Table S1). Solutions from the peak fractions were stable upon isolation, and had low polydispersity and a hydrodynamic radius ranging from 2.89–3.82 nm by dynamic light scattering (DLS) (Fig. 1*C*, Table S1). We used fluorescent lipids with SEC and thin layer chromatography to confirm that phosphotidylcholine (PC), phosphatidylinositol (PI), bis(monoacylglycero)phosphate (BMP), cholesterol, galactosylceramide (GalCer), and sphingomyelin (SM) could be incorporated into the 3.2-nm saposin A lipoproteins (Fig. 1*D*). Using liposomes made from pure egg PC, we purified 3.2-nm particles by SEC and determined the protein and lipid concentrations by quantitative amino acid analysis and a phosphorus content assay, respectively. The 3.2-nm particles contained a ratio of 5 ± 1 lipid molecules per saposin A chain. Given the narrow and unimodal distribution of particle sizes, we propose that the 3.2-nm PC complexes contain two copies of saposin A and 8 to 12 lipids.

Crystal Structure of a Saposin A/Detergent Disc. We attempted to crystallize saposin A with a variety of lipids, including glycosphingolipids, phospholipids, and detergents, and obtained X-ray diffraction quality crystals with the detergent LDAO. We were able to solve the structure by sulfur single-wavelength anomalous diffraction (SAD) phasing, because the high sulfur content in saposin A (nine sulfur atoms per chain) gave a robust anomalous signal for high redundancy datasets collected with Cr Kα radiation. The model was refined against a 1.9-Å resolution dataset collected with higher energy X-rays. Data collection and refinement statistics are given in Table S2.

The crystal structure revealed an open saposin fold in which the stem and hairpin segments of the protein are opened in a jackknife fashion relative to the closed form of the protein (Fig. 2). A comparison of the lipid-free closed form of saposin A (15) and LDAO-bound open form reveal that the main structural rearrangements in the protein involve residues 19–23 and 62–69. These two regions form the hinges that allow the stem and hairpin segments of saposin A to open up into a V shape, resulting in an opening of approximately 115° between the two halves of the protein. Residues 62–67 are in a coil conformation in the closed form, but extend the C-terminal end of helix α3 in the open form. There are only minor conformational changes near residue Y54, which is an important hinge residue in saposins B and C (3, 18, 19). Structures of saposin C have been observed in two open states: as a dimeric homodimer with no associated lipid (18) and in association with SDS micelles by NMR (19). In the latter study, no information about the structure of the bound detergent or the overall assembly of the saposin C/SDS complex could be determined.

The open state of the protein exposes a concave hydrophobic inner face, and this surface is covered by LDAO acyl chains in the crystal structure (Fig. 3). Two V-shaped protein chains face each other and form a ring around a detergent minibilayer (Fig. 4). Thus, the protein-detergent complex is comprised of an external protein belt that surrounds a cluster of 40 internalized and well-ordered detergent molecules (Fig. S2). This observation is in contrast to what is seen in protein-detergent complexes of integral membrane proteins, which have an inner protein core surrounded by externally bound and largely disordered detergent molecules. Notably, there are no saposin-saposin contacts in the assembly, and the particle is held together entirely by the deter-

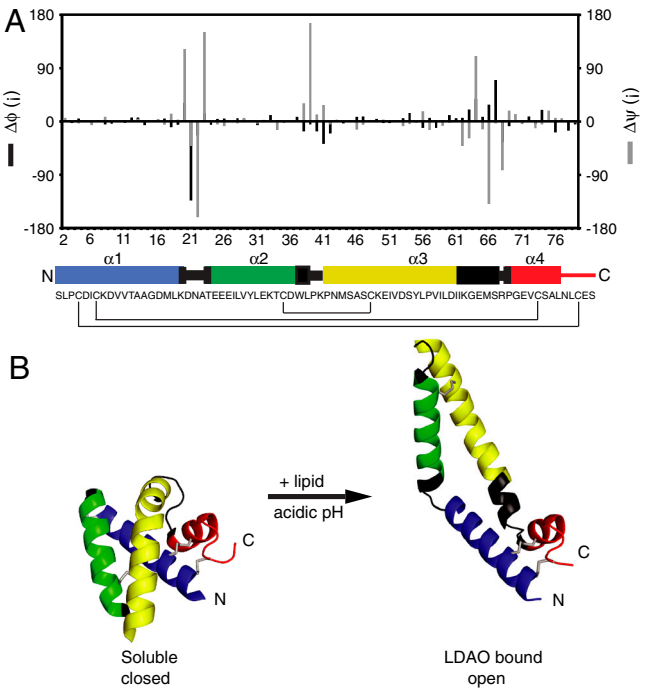

Fig. 2. Conformational analysis of saposin A in the closed form [soluble apo; Protein Data Bank (PDB) ID code 2DOB] compared to the open form (LDAO complex, this work). (*A*) Differences in the main chain torsion angles between the apo and LDAO complexes. The residues with significant conformational changes are shown in black in the secondary structure schematic of the protein. The thin lines connecting cysteine residues represent disulfide bonds. (*B*) Ribbon diagram of the two forms, with the stem region (helices α1 and α4) in the same orientation in both views. Coloring as in *A*.

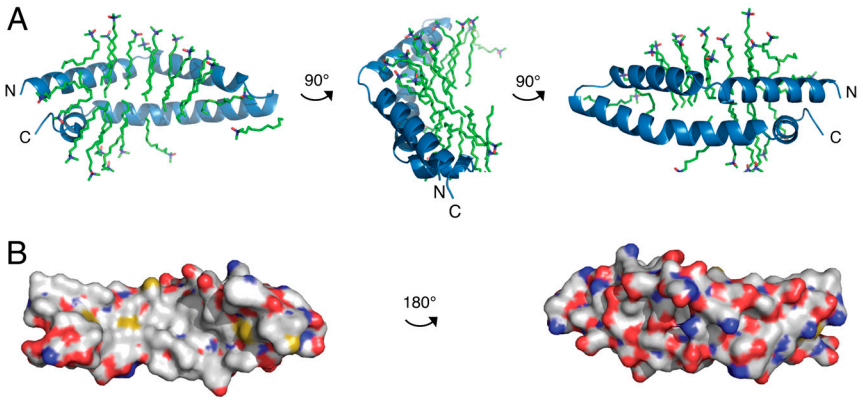

Fig. 3. Crystal structure of saposin A in complex with LDAO. (*A*) Three views of the half dimer seen in the crystal asymmetric unit. Saposin A is shown in blue ribbons with the 20 LDAO molecules rendered with red oxygens, dark blue nitrogens, and green carbons. (*B*) Surface representations of the open form of saposin A from the crystal structure showing the apolar concave surface and polar convex surface. Carbons are colored white. The detergent molecules are not included in this representation.

gent hydrophobic core. This arrangement differs from the situation seen with the saposin B dimer, in which extensive protein-protein contacts between two open-form chains with hinge openings with an angle of approximately 70° form a stable protein shell. The saposin B protein shell can accommodate a small number of enclosed lipids with only a small opening for lipid head group exposure (Fig. S3) (3). In contrast, the amphiphile head groups make up approximately 35% of the surface area of the saposin A/LDAO assembly. The overall saposin A lipoprotein complex is reasonably described as an elliptic cylinder with a height of 33 Å and major and minor semiaxes of 56 and 41 Å.

As a result of the high surface area to volume ratio of the open state, 36 of the 81 saposin A side chains are involved in protein-detergent contacts. Of these, 18 are either leucine, isoleucine, or valine residues. The remaining amino acids are also nonpolar residues, with the exception of T23, T34, and E65. The latter amino acid is probably protonated, based on the geometrical arrangement of residues E65, R68, and E71 which form a hydrogen-bonded network at the $\alpha 3/\alpha 4$ loop. This segment may be important in determining the pH dependent properties of this saposin.

Aromatic residues Y30 and W37 face the detergent core and are nestled between LDAO molecules near the water-lipid interface (Fig. 5), consistent with the observed changes in the tryptophan emission spectrum induced by either detergent or lipid (Fig. 1*A*). Aromatic residues are often found in the bilayer interface region of integral membrane proteins (22) and this effect may also be present in saposin A lipid complexes.

Disc Asymmetry. The complex has a twofold symmetry axis normal to the plane of the disc, but there are no twofold rotational symmetries in the plane of the membrane. As a result, the upper surface of the lipoprotein disc is not equivalent to the lower surface. The top surface of the saposin A disc is framed by helix α2 and is open and wide, whereas the bottom α4 face is smaller and has a less regular arrangement of LDAO (Fig. 4 *B* and *C*). There are 24 detergent molecules in the upper leaflet and 16 LDAO molecules in the lower leaflet. The asymmetry in the saposin A lipoprotein discs might have direct functional consequences in the galactosylceramide hydrolysis activation reaction if we assume that the productive presentation of the target lipid to the enzyme in a saposin A lipoprotein complex occurs exclusively on either the upper or lower face of the disc.

Structure of the Acyl Core. The complex is held together by the detergent core and there are no direct protein-protein contacts in the dimer. Approximately 80% of the 360 detergent acyl chain dihedral angles in the saposin A complex are in the *trans* conformation. A slab in the plane of the disc near the C8 atoms in the upper LDAO leaflet reveals the densest and most regular part of the acyl chain packing. In this region, the chains pack into a pseu-

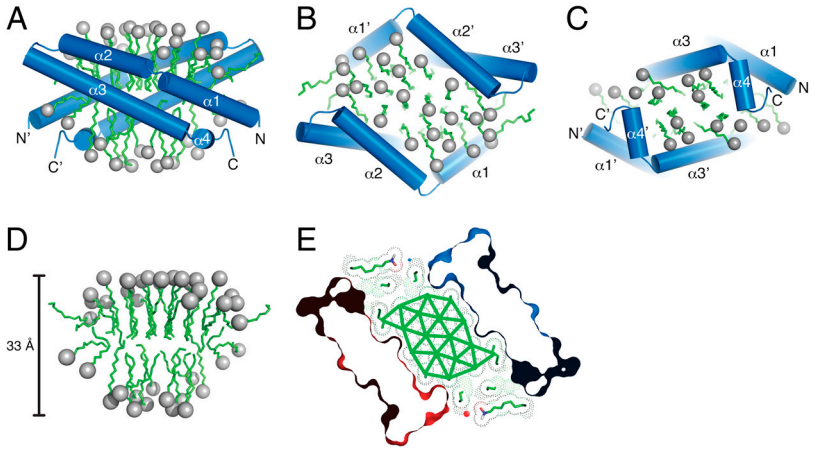

Fig. 4. Structure of the saposin A/LDAO lipoprotein discs. (*A*) Side view of the complex. (*B*) View from the top of the dimer (relative to *A*). (*C*) View from the bottom of the dimer. The LDAO head groups are represented by gray spheres. (*D*) Assembly of the 40 LDAO molecules from the dimer. The view is similar to the view as in *A*, but without the protein. (*E*) A thin slab in the region of the C8 atoms of the upper LDAO leaflet reveals a pseudohexagonal lattice involving 18 detergent molecules. The two saposin A monomers are represented as red and blue surfaces, and the detergent molecules are shown in stick representation with dotted van der Waals surfaces. Green lines connect the detergent pseudoatomic positions in the projection.

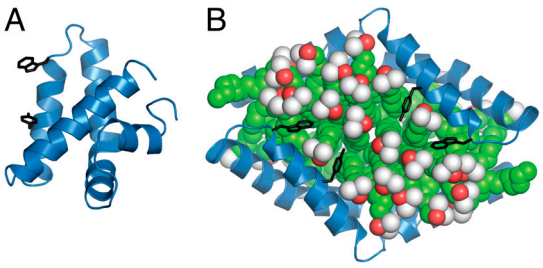

Fig. 5. Differences in the environment of the aromatic residues in helix α2. (*A*) Residues Phe30 and Trp37 (black) are solvent exposed in the apo form of saposin A. (*B*) The side chains are buried in the LDAO head group/acyl chain interface region in the complex. This view is from the same perspective as in Fig. 4*B*.

dohexagonal lattice with a surface area of approximately 21 Å^2 per hydrocarbon chain (Fig. 4*E*, Fig. S4), similar to the expected value for crystalline hexagonal saturated hydrocarbon chain packing (23). The average length between the pseudoatomic positions in the lattice (Fig. 4*E*) is 4.9 ± 0.4 Å, in close agreement with the ideal value of 4.85 Å (23). There are no waters in the interior of the complex, and the semicrystalline packing of the acyl chains is the result of filling a defined volume with a near-maximal amount of lipid. This volume is dictated by the shape of the protein shell, which is constrained to defined geometries as it adapts to the internalized lipids.

Coarse-Grained Molecular Dynamics Simulations. We next asked whether the saposin A/LDAO structure comprised of single chain amphiphiles with C12 tails is a suitable model for the 3.2-nm lipoprotein particles containing, for example, diacyl tails with 16 to 20 carbons. Notably, 40 LDAO molecules have approximately the same mass as 8–12 PC lipids that we expect in a dimeric saposin A/lipid complex. Thus, both a 40:2 LDAO:saposin A complex and a 10:2 phospholipid:saposin A complex have masses of approximately 27 kDa.

We used molecular dynamics to study the simplest saposin A/lipid system, which is saposin A with PC. We performed an unconstrained modeling study of saposin A/1-palmitoyl-2-oleoyl-sn-glycero-3-phosphocholine (POPC) lipid complexes with 250 parallel coarse-grained simulations. A range of configurations were generated and we selected the simulations with the closest configurations to that of the crystal structure for further analysis (*SI Text*, Figs. S5–S7, Table S3).

The protomers in these simulations are arranged in a similar configuration as the crystal structure (Fig. 6*A*). As with the LDAO structure, the methylene groups of the lipid tails are held within the central cavity of the complex, where they interact with the hydrophobic faces of the saposin A protomers (Fig. 6 *B* and *C*). Outside of this region, the POPC head groups form a corona that completes the polar surface of the assembly. A representative snapshot of the lipids reveals that the lipids are arranged in two leaflets as a minibilayer (Fig. 6*C*), similar to what is seen in the LDAO structure. Consistent with the LDAO crystal structure, we observed an asymmetric distribution of POPC molecules, with more lipid molecules favored in the upper versus lower leaflets (Fig. 6*D*).

Overall, these simulations are consistent with our experimental results but do not prove that the 3.2-nm lipidic particles that we observe experimentally correspond to the saposin A/LDAO crystal structure. Because the crystal structure is one static view of the complex, additional configurations for the assemblies may occur with LDAO or with lipids.

Similarities to High Density Lipoproprotein (HDL) Particles. The hinge opening mechanism in the saposin proteins has similarities with the conformational changes seen in the apolipoproteins in discoidal HDLs, but the commonly accepted double belt model

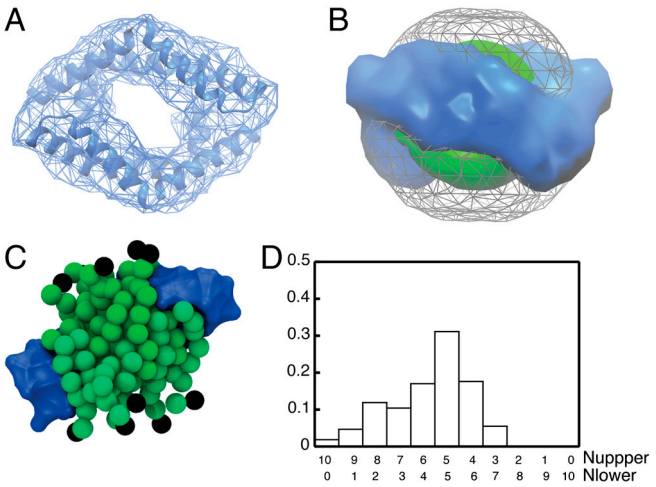

Fig. 6. Structural features of a POPC containing saposin A-lipid disc from coarse-grained simulations. (*A*) The saposin A crystal structure is shown in ribbon representation superimposed over the spatial distribution of the protein from the simulations (wire mesh). Top view of the disc. (*B*) Side view of the saposin A-lipid disc from the simulations. The protein spatial distribution is shown in solid blue surface, the POPC tails are in solid green surface, and the POPC choline head group distribution is in gray wire frame. (*C*) Snapshot of a representative structure from the coarse-grained simulation. The choline head group of the lipid is represented by a black bead, and the acyl chains of the two POPC leaflets are colored in different shades of green. The molecular surface of one of the saposin A chains is shown in blue. The frontmost saposin A chain is omitted to reveal the lipidic core of the complex. (*D*) Leaflet distribution of POPC molecules shown by the time series histogram of the number of POPC molecules in the upper (N_{upper}) and lower (N_{lower}) leaflet in the 33 representative simulations.

for discoidal HDLs proposes two stacked antiparallel ring-shaped protein monomers (24–26). In the case of the saposin A complexes, a head-to-tail arrangement of two subunits is observed, with the two disulfide-linked helices of the stem and hairpin regions forming the width of the belt. Superficially, this saposin A arrangement resembles a hairpin model proposed for apolipoprotein A-I HDLs (27). In the case of both saposin A and HDL particles, the number of protein subunits, their relative orientation, and the helix-helix hinge opening angles determine the size and shape of the discs. Given the relatively narrow size distributions that we have observed with the 3.2-nm particles (Fig. 1), the saposin A lipoprotein particles appear to be limited to two protein subunits. Overall, relative to the HDL apolipoproteins, saposin A is a more rigid molecule and forms much smaller lipid complexes.

Conclusions

The saposin A/lipid disc is most likely the effective substrate-presenting particle in galactosylceramide hydrolysis. We propose that saposin A activates the galactosylceramide hydrolysis reaction by solubilizing the target lipid in 3.2-nm particles, thus increasing the accessibility of the lipid head group to the enzyme active site. In addition to providing insight into the mechanism of the glycosphingolipid activation reaction, saposin A lipoproteins may have practical applications in other areas. For example, by analogy with engineered apolipoprotein complexes (25), small, stable saposin A lipoprotein complexes may find unique technological applications.

Materials and Methods

Crystallization and Structure Determination. Saposin A was expressed and purified as previously reported (15) (*SI Text*). Crystals were grown at room temperature by vapor diffusion using the hanging drop method by mixing 1 μL of 5 mg/mL saposin A containing 25 mM LDAO with 1 μL of reservoir solution containing 1.6 M trisodium citrate pH 6.5. Crystals formed in space group $P6_122$ with unit cell dimensions $a = b = 39.8$ Å and $c = 247.3$ Å. Native

diffraction data were collected at 100 K at beamline 19-ID at the Advanced Photon Source at the Argonne National Laboratory and reduced with the HKL package (28). The same crystal was subsequently used to collect a 2.5 Å anomalous dataset on a Rigaku FR-E+ Superbright X-ray generator with a Cr anode, VariMax Cr optics and a Raxis IV++ detector at the Structural Genomics Consortium. The structure was solved by S-SAD phasing with the Cr data using the SHELXC/D/E suite of programs (29). The positions of eight of the nine sulfur atoms in saposin A were located in the initial substructure by SHELXD using the DSUL disulfide resolution option, and 79 of the 80 protein residues were automatically traced as a polyalanine model by SHELXE. Final model building and refinement were carried out using the high-resolution synchrotron dataset with ARP/wARP (30), REFMAC5 (31), and Coot (32). Protein structure images were produced with PyMOL (33).

Coarse-Grained Molecular Dynamics Simulations. Simulations were performed with the GROMACS simulation package, version 4.0 (34) with the MARTINI CG force field, version 2.0 (35, 36) (*SI Text*). A coarse-grained representation of the saposin A protomers was created and two monomers were randomly oriented and positioned in the simulation box. Separately, an aggregate of 10 POPC lipids was randomly positioned in the box. The system was then solvated by replication of an equilibrated coarse-grained water box containing 10,800 water interaction centers, followed by the addition of 150 mM sodium chloride. The final system contained approximately 14,500 pseudoatoms. Unfavorable contacts created in the set up procedure were removed by energy minimization using the steepest descent algorithm. Simulations were performed for a nominal time of 1 μs, with a time step of 20 fs. A total of 250 independent simulations were performed using different random seeds to generate the initial configurations and in the velocity assignments. Similar results were obtained at POPC:saposin ratios of 8:2 and 12:2.

ACKNOWLEDGMENTS. We thank the Advanced Photon Source at the Argonne National Laboratory for access to synchrotron facilities and Aiping Dong at the Structural Genomics Consortium Toronto for help with the Cr X-ray dataset. Computations were performed on the General Purpose Cluster supercomputer at the SciNet High Performance Computing Consortium. SciNet is funded by the Canada Foundation for Innovation under the auspices of Compute Canada, the Government of Ontario, Ontario Research Fund—Research Excellence, and the University of Toronto. This work was supported by Canadian Institutes of Health Research (CIHR) grants (G.G.P. and R.P.); a Natural Sciences and Engineering Research Council of Canada grant (G.G.P.); a CIHR Frederick Banting and Charles Best Canada Graduate Scholarship (K.P.); a CIHR Training Program in Protein Folding and Interaction Dynamics (J.H.); and a Canada Research Chairs Program chairholder (R.P.). This research was funded in part by the Ontario Ministry of Health and Long Term Care.

1. Kolter T, Sandhoff K (2010) Lysosomal degradation of membrane lipids. *FEBS Lett* 584:1700–1712.
2. Wendeler M, et al. (2004) Photoaffinity labelling of the human GM2-activator protein. Mechanistic insight into ganglioside GM2 degradation. *Eur J Biochem* 271:614–627.
3. Ahn VE, Faull KF, Whitelegge JP, Fluharty AL, Privé GG (2003) Crystal structure of saposin B reveals a dimeric shell for lipid binding. *Proc Natl Acad Sci USA* 100:38–43.
4. Alattia JR, Shaw JE, Yip CM, Privé GG (2007) Molecular imaging of membrane interfaces reveals mode of beta-glucosidase activation by saposin C. *Proc Natl Acad Sci USA* 104:17394–17399.
5. O'Brien JS, et al. (1988) Coding of two sphingolipid activator proteins (SAP-1 and SAP-2) by same genetic locus. *Science* 241:1098–1101.
6. Furst W, Sandhoff K (1992) Activator proteins and topology of lysosomal sphingolipid catabolism. *Biochim Biophys Acta* 1126:1–16.
7. Yamada M, et al. (2004) Analysis of recombinant human saposin A expressed by *Pichia pastoris*. *Biochem Biophys Res Commun* 318:588–593.
8. Harzer K, et al. (1997) Saposins (sap) A and C activate the degradation of galactosylceramide in living cells. *FEBS Lett* 417:270–274.
9. Matsuda J, Vanier MT, Saito Y, Tohyama J, Suzuki K (2001) A mutation in the saposin A domain of the sphingolipid activator protein (prosaposin) gene results in a late-onset, chronic form of globoid cell leukodystrophy in the mouse. *Hum Mol Genet* 10:1191–1199.
10. Spiegel R, et al. (2005) A mutation in the saposin A coding region of the prosaposin gene in an infant presenting as Krabbe disease: First report of saposin A deficiency in humans. *Mol Genet Metab* 84:160–166.
11. Suzuki K (2003) Globoid cell leukodystrophy (Krabbe's disease): Update. *J Child Neurol* 18:595–603.
12. Wenger DA, Rafi MA, Luzi P, Datto J, Costantino-Ceccarini E (2000) Krabbe disease: Genetic aspects and progress toward therapy. *Mol Genet Metab* 70:1–9.
13. Darmoise A, Maschmeyer P, Winau F (2010) The immunological functions of saposins. *Adv Immunol* 105:25–62.
14. Zhou D, et al. (2004) Editing of CD1d-bound lipid antigens by endosomal lipid transfer proteins. *Science* 303:523–527.
15. Ahn VE, Leyko P, Alattia JR, Chen L, Privé GG (2006) Crystal structures of saposins A and C. *Protein Sci* 15:1849–1857.
16. Bruhn H (2005) A short guided tour through functional and structural features of saposin-like proteins. *Biochem J* 389:249–257.
17. Popovic K, Privé GG (2008) Structures of the human ceramide activator protein saposin D. *Acta Crystallogr D Biol Crystallogr* 64:589–594.
18. Rossmann M, et al. (2008) Crystal structures of human saposins C and D: Implications for lipid recognition and membrane interactions. *Structure* 16:809–817.
19. Hawkins CA, de Alba E, Tjandra N (2005) Solution structure of human saposin C in a detergent environment. *J Mol Biol* 346:1381–1392.
20. Locatelli-Hoops S, et al. (2006) Saposin A mobilizes lipids from low cholesterol and high bis(monoacylglycerol)phosphate-containing membranes: Patient variant Saposin A lacks lipid extraction capacity. *J Biol Chem* 281:32451–32460.
21. Vaccaro AM, et al. (1995) pH-dependent conformational properties of saposins and their interactions with phospholipid membranes. *J Biol Chem* 270:30576–30580.
22. Killian JA, von Heijne G (2000) How proteins adapt to a membrane-water interface. *Trends Biochem Sci* 25:429–434.
23. Small DM (1984) Lateral chain packing in lipids and membranes. *J Lipid Res* 25:1490–1500.
24. Hatters DM, Peters-Libeu CA, Weisgraber KH (2006) Apolipoprotein E structure: Insights into function. *Trends Biochem Sci* 31:445–454.
25. Nath A, Atkins WM, Sligar SG (2007) Applications of phospholipid bilayer nanodiscs in the study of membranes and membrane proteins. *Biochemistry* 46:2059–2069.
26. Thomas MJ, Bhat S, Sorci-Thomas MG (2008) Three-dimensional models of HDL apoA-I: Implications for its assembly and function. *J Lipid Res* 49:1875–1883.
27. Tricerri MA, Behling Agree AK, Sanchez SA, Bronski J, Jonas A (2001) Arrangement of apolipoprotein A-I in reconstituted high-density lipoprotein disks: An alternative model based on fluorescence resonance energy transfer experiments. *Biochemistry* 40:5065–5074.
28. Otwinowski Z, Minor W (1997) Processing of X-ray diffraction data collected in oscillation mode. *Meth Enzymol* 276:307–326.
29. Sheldrick GM (2010) Experimental phasing with SHELXC/D/E: Combining chain tracing with density modification. *Acta Crystallogr D Biol Crystallogr* 66:479–485.
30. Langer G, Cohen SX, Lamzin VS, Perrakis A (2008) Automated macromolecular model building for X-ray crystallography using ARP/wARP version 7. *Nat Protoc* 3:1171–1179.
31. Murshudov GN, Vagin AA, Dodson EJ (1997) Refinement of macromolecular structures by the maximum-likelihood method. *Acta Crystallogr D Biol Crystallogr* 53:240–255.
32. Emsley P, Lohkamp B, Scott WG, Cowtan K (2010) Features and development of Coot. *Acta Crystallogr D Biol Crystallogr* 66:486–501.
33. DeLano WL (2002) The PyMol Molecular Graphics System. (DeLano Scientific, San Carlos, CA).
34. Hess B, Kutzner C, van der Spoel DLE (2008) GROMACS 4: Algorithms for highly efficient, load-balanced, and scalable molecular simulation. *J Chem Theory Comput* 4:435–447.
35. Marrink SJ, Risselada HJ, Yefimov S, Tieleman DP, de Vries AH (2007) The MARTINI force field: Coarse grained model for biomolecular simulations. *J Phys Chem B* 111:7812–7824.
36. Monticelli L, et al. (2008) The MARTINI coarse-grained force field: Extension to proteins. *J Chem Theory Comput* 4:819–834.